Journal of the Korean Nuclear Society
Vol. 3, No. 2, June, 1971

≪Original≫

Shielding Effectiveness of Magnetite Heavy Concrete on Cobalt-60 Gamma-rays

Yong Kyu Lim

Health Physics Division, Atomic Energy Research Institute

(Received April 15, 1971)

Abstract

The gamma-ray shielding effects of magnetite concretes have been measured using a broad beam Co-60 gamma-ray source. Mathematical formulae for a transmission ratio-to-shield thickness relation were derived from the attenuation curve obtained experimentally and are

$I_{(X)}=I_{(o)}\exp(-\mu X)\exp(1.03\times10^{-1}X-3.38\times10^{-3}X^2+5.29\times10^{-5}X^3)$ when $X<20$ cm,

$I_{(X)}=I_{(o)}\exp(-\mu X)\exp(4.66\times10^{-2}X+2.12\times10^{-1})$ when $X>20$ cm.

Here $I_{(X)}$ is radiation intensity after passing through a thickness X of absorber, $I_{(o)}$ is the initial radiation intensity, μ is the linear attenuation coefficient of magnetite concrete and is given by $(0.0532\rho+0.0083)^{4)}$ cm^{-1} in accordance with an earlier study, and X is the thickness of absorber. In addition, a model shield which is a rectangular magnetite concrete box with walls of 8 cm thickness walls and internal demensions of $40\times40\times40$ cm was constructed and its shielding effect has been measured. The emergent radiation flux appears to be greater with this configuration than with a slab shield of equal thickness.

요 약

국내에서 산출되는 각종 광물골재를 사용하여 방사선 차폐용 중차폐 콩크리트를 제조하고 감마선에 대한 차폐 효과를 실험한 결과 최적하다고 판단된 자철광 중차폐 콩크리트를 대상으로 ^{60}Co 감마선의 Broad beam을 사용하여 방사선 차폐 효과를 측정하였다. 본 실험을 통하여 실험적으로 차폐체내의 방사선의 감쇄곡선으로부터 차폐체 두께의 변화에 따르는 방사선 투과율과의 상호관계에 관한 수식을 다음과 같이 유도해냈다.

$I_{(X)}=I_{(o)}\exp(-\mu X)\exp(1.03\times10^{-1}X-3.38\times10^{-3}X^2+5.29\times10^{-5}X^3)$ $X<20$ cm 때,

$I_{(X)}=I_{(o)}\exp(-\mu X)\exp(4.66\times10^{-2}X+2.12\times10^{-1})$ $X>20$ cm 때.

이와같이 얻은 결과식에서 오른쪽 첫번째항은 최초 감마선의 감쇄를 표시하고 그 다음항은 차폐체 내에서의 감마선 재생계수를 나타낸다.

이 실험에 첨가하여 차폐체의 실제 설계에 입각한 입방형 자철광 구조체 (두께 8 cm, 내부공간 $40\times40\times40$ cm)에 대한 차폐효과를 측정한 결과 평판 차폐체를 사용할때보다 투과 방사선이 증가됨을 알았다.

1. Introduction

The gamma-ray shielding could be calculated by the theoretical approach, which begins with interaction cross sections. The validity, however, becomes less reliable with increasing shield thickness.[1] Alternatively it can be often made by experiments which are concerned with the total effect on attenuation and build-up factors.[2] The latter yields generally more useful data for the practical application than the former, although the latter gives only gross results. Unfortunately, the experimental data obtained for a shielding material cannot be used extensively for other shielding material. Therefore, measurements of attenuation coefficient and build-up factors are necessary if there are no appropriate data obtained experimentally for any shielding material.

A number of experimental data[3] are published for lead, iron, water, aluminum, ordinary concrete and so on, but for magnetite concrete which is readily and economically available in domestic market data are not available

The purpose of this paper is to obtain experimentally the attenuation coefficients and build-up factors of the slab magnetite heavy concrete for ^{60}Co gamma-rays.

The gamma-ray shielding effects of heavy concretes manufactured with ten different mineral ores produced domestically were investigated in the previous work[4] by the author. That study, which evaluates material cost as well as shield effectiveness, indicated that magnetite heavy concrete would be the most promising material for a biological shield of gamma-rays. In the present study, the gamma-ray attenuation properties of this magnetite concrete were studied in detail. The samples used in this study were formed into slabs with demensions of $40\times40\times8$ cm. The measurements of uniformity and gamma-ray attenuation coefficient for the test specimens were carried out by means of the gamma-ray transmission method. The broad beam from a 3.2 mCi Co-60 point source was used and the spectra as well as the fluxes of the emergent photons were measured by means of Scintillation detector and 400 multi-channel analyzer. Variations on spectra and fluxes of the emergent radiation were measured as the shield thickness was changed. From the experimental results, important factors such as attenuation coefficients, half value layer, build up factor which should be considered in designing biological shield were determined. Also a mathemetical expression governing the relation between the transmission ratio and thickness of concrete shielding was derived from the curve fitting of the experimental data.

2. Experimental Procedure

2-1. Choice of Aggregates

A biological shield must provide adequate protection for personnel at a reasonable cost. There are many factors, e.g., shielding effectiveness, shield density and composition, structural strength, which may influence the design of a biological shield.

The most effective gamma-ray shielding requires material with a specific gravity as high as possible. If shielding effect only is considered, materials with high atomic numbers should be employed. However, such material can not be used for general purposes because of their high cost. Materials for a biological shield, therefore, must be chosen considering both shielding effect and economy.

The shielding effects of various mineral ores which are produced in the different domestic mines were examined in the previous study.[4] Among them, magnetite ore produced in the Pochun mine near Seoul was believed to be the best material for a gamma-ray shield from

Table 1. Physical chemical properties of magnetite ore from the Pochun mine.

Samples	Ore-size (mm)	Specific Gravity (g/cm^3)	Water Absorption (%)	*Chemical Analysis (%)							
				Fe	FeO	Fe_2O_3	SiO_2	S	SO_3	CaO	MgO
Mag. —A	40~20	4.27	0.60	(53.59)* 0.35	22.72	50.80	9.82	0.16	0.00	—	—
Mag. —B	20~5	4.19	0.63	(54.05)* 0.40	23.29	50.77	12.56	trace	0.00	2.12	0.81
Mag. —C	> 5	4.12	0.66	(54.81)* 0.26	24.14	51.10	11.80	〃	0.00	2.26	0.81
Mag. —D	>0.42	4.10	0.71	(53.79)* 0.24	24.06	49.77	10.02	〃	0.00	1.41	2.24

* Chemical analysis was done by the Geological Survey of Korea.
( )* Total iron in ore, includes free iron plus that in FeO, Fe_2O_3.

the criteria, mentioned above. Table 1, Pochun magnetite is an iron ore which contains predominantly an iron oxide, resulting in a high specific gravity.

In addition, ores from the Pochun mine can be readily transported since this mine is located near Seoul. For these reasons, magnetite ore produced in Pochun was chosen for a detailed study of the gamma-ray shielding effectiveness.

2-2. Experimental Arrangement

The photon interacts with the particles of the test sample (or with the electromagnetic fields associated with these particle)in such a manner that the original photon is lost. Through the interaction with these particles, secondary photons are produced by photoelectic effect, Compton scattering or pair production. These secondary photons have less energy than that of the primary photon, and have a directional distribution.[5] As a result, photons emerging from the shield have a wide energy and spatial distribution. This means that every spot-measurements of the radiation flux and its energy distribution at the shield surface in question are necessary to design the biological shield.

Although it is very desirable to carry out these measurements, it is not usually possible to perform such laborious experiments,

In view of the radiation protection, it is common to design the biological shield with the consideration of maximun radiation flux emerging from the shield surface. The maximum emergent flux, which consists of the scattered and primary radiation, mainly occurs in the same axis as the direction of primary radiation.[5, 6]

For these reasons, both 3.2 mCi Co-60 gamma-ray source and the measuring instrument were installed on the same axis. The test sample was placed perpendicularly with regard to the detector. A broad beam source was used in this experiment, and the spectra as well as the fluxes of the emergent photons were measured by means of a 400 channel pulse height analyzer(Hitachi, model RAH-403) coupled with a NaI(Tl) crystal of 3 in. diameter by 3 in. long. In this way, variations on spectra and fluxes of the emergent radiation were measured as the shield thickness was changed. During a day's run of this multichannel analyzer, the pulse height corresponding to a given photon energy of 1.17 Mev showed less than a 1% variation. Fig. 2 shows a schematic diagram for the experimental arrangement used in the work.

In addition, a model shield was constructed and its shielding effect was measured. This model shield was a rectangular concrete box

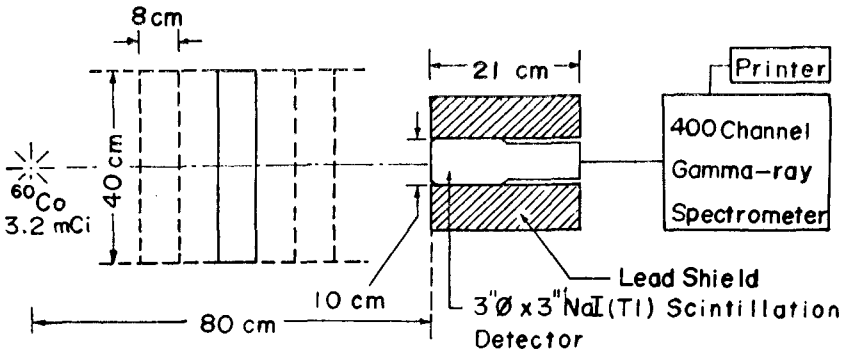

Fig. 2. Schematic diagram for apparatus and experimental arrangement.

with an internal space of 40×40×40 cm and shield thickness of 8 cm. A 3.2 mCi Co-60 gamma-ray source was put in the center of the box and the measurements of the emergent radiation were carried out by the same method as described before. The model shield chosen here is not practical to give the useful data for the practical shield design, but as a preliminary study for the simple shield geometry, this experiment was performed.

2-3. Magnetite-Concrete Design and Its Uniformity Test

Sample heavy concretes were mixed using magnetite as an aggregate, after considering the water-to-cement ratio(or the W/C ratio where W is the water content and C is the cement content) of various materials which is closely related to the workability and the

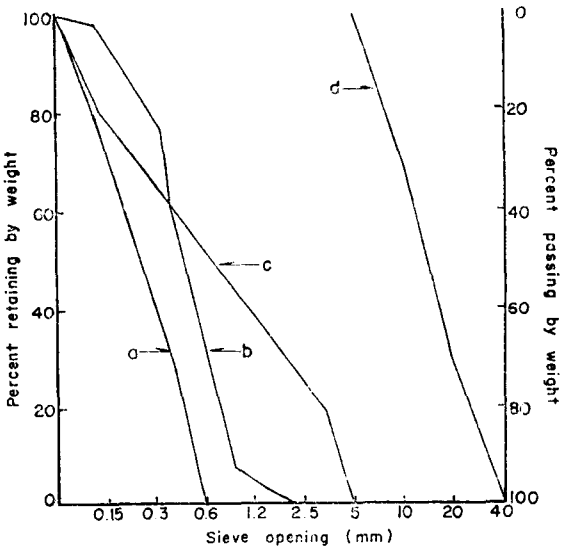

a: Magnetite fine grain, b;Sand (Han-river)
c: Magnetite fine aggregate
d: Magnetite coarse aggregate and gravel(Han-river)

Fig. 1. Results of sieve analysis for the aggregates used in samples.

Table 2. Experimental data on the concrete combination.

Sample Number	Aggregates		Materials in 1m³ of concrete (kg)				Water-Cement Ratio (%)	S/A Ratio (%)	Slump (cm)	Compressive strength** (kg/cm²)
	Fine	Coarse	Cement	Water	Fine Agg.	Coarse Agg.				
M-1~M-7	Mag. Fine Agg. *(c)	Mag. Coarse Agg. (d)	324	165	1,024	1,987	51	34	3.1	210
M-8, M-9	Mag. Fine Grain (a)	Mag. Coarse Agg. (d)	322	164	1,026	1,992	51	34	2.9	200
SM-1	Sand (b)	Mag. Coarse Agg. (d)	306	168	640	1,994	55	34	2.5	180
SM-2	Sand (b)	Mag. Coarse Agg. (d)	283	170	624	2,009	60	34	3.0	163
MG-1	Mag. Fine Agg. (c)	Gravel (d)	325	166	1,052	1,236	51	35	2.0	180
MG-2	Mag. Fine Agg. (c)	Cravel (d)	325	166	1,953	666	51	65	1.5	105

*( ) Denotes appropriate aggregate grain curve from Fig. 1.
** Obtained from the test concrete samples cured in water at 20°C, 28 days.

structural strength of the concrete manufactured.

In order to get the concrete with a density as high as possible, magnetite aggregate with the optimum graded form as determined in the previous work[4] was used.

Figure 1 presents the results of sieve analysis for the aggregates, while Table 2 gives the experimental data on concrete combination of the various samples. Items (a), (b), (c) and (d) appearing in columns two and three of the table specify the appropriate aggregate grain-size curve from Figure 1. The water-to-cement(W/C) ratio is closely related to the workability and structural strength of the resulting concrete. The S/A ratio specifies the percentage of the total aggregate formed by the fine aggregate. The obtained from test specimens cured in water at 20°C for 28 days.

The samples used in this study were formed into slabs with dimensions of 40×40×8 cm.

The dimensions of the test specimens were selected after considering the detector geometry and the Co-60 activity to be used in the experiment. The thickness of 8 cm was chosen to assure concrete with the desired structural strength and uniformity, since the coarse aggregates included grains up to 4 cm in diameter.

The measurements of uniformity and gamma-ray attenuation coefficient were carried out by means of the gamma-ray transmission method. To determine specimen uniformity, the lateral (40×40cm) surface of the sample was sectioned at 5 cm intervals. At each of the 49 interior mesh points, photons from a collimated Co-60 gamma ray beam of 5 mm diameter, which penetrating the specimen were measured with a typical narrow beam detecting system consisting of an electronic decade scaler(Nuclear Chicago Co., model 181 A) coupled to a 2 in. diameter by 2 in. long thallium-activated sodium iodide crystal in an appropriate lead shield. Collimating hole in the detector shield had a diameter of 13 mm that of the source, but was selected to improve the detection

Table 3. ***Summary of the gamma-ray transmission experiment.**

Sample Number	Aggregates		Transmission Ratio	Linear-Absorption Coefficient μ (cm^{-1})	Subdued Length (1/e-Value) (cm)	Half-Value Length (cm)	1/10-Value Length (cm)	Mass Absorption Coeff. μ_m (cm^2/g)	Measured Density g/cm^3	**Deviation rate for uniformity (%)
	Fine	Coarse								
M—1	Mag. Fine Agg.	Mag. Coarse Agg.	0.2067	0.1954	5.12	3.55	11.79	0.0558	3.50	6.85
M—2	Mag. Fine Agg.	Mag. Coarse Agg.	0.2108	0.1940	5.15	3.57	11.87	0.0552	3.52	5.42
M—3	Mag. Fine Agg.	Mag. Coarse Agg.	0.2044	0.1977	5.06	3.51	11.65	0.0567	3.49	6.01
M—4	Mag. Fine Agg.	Mag. Coarse Agg.	0.2065	0,1966	5.07	3.52	11.71	0.0563	3.50	4.72
M—5	Mag. Fine Agg.	Mag. Coarse Agg.	0.2148	0.1913	5.23	3.62	12.04	0.0550	3.48	5.97
M—6	Mag. Fine Agg.	Mag. Coarse Agg.	0.2119	0.1920	5.21	3.61	12.00	0.0551	3.48	7.38
M—7	Mag. Fine Agg.	Mag. Coarse Agg.	0.2087	0.1958	5.11	3.54	11.76	0.0569	3.44	6.29
M—8	Mag. Fine Grain	Mag. Coarse Agg.	0.2059	0.1924	5.20	3.60	11.97	0.0556	3.46	4.21
M—9	Mag. Fine Grain	Mag. Coarse Agg.	0.2035	0.1961	5.10	3.53	11.74	0.0565	3.47	6.83
SM—1	Sand	Mag. Coarse Agg.	0.2595	0.1682	5.95	4.12	13.69	0.0566	2.97	12.83
SM—2	Sand	Mag. Coarse Agg.	0.2451	0.1742	5.80	3.98	13.22	0.0583	2.99	10.02
MG—1	Mag. Fine Grain	Gravel	0.2721	0.1599	6.25	4.33	14.40	0.0586	2.73	7.30
MG—2	*Mag. Fine Grain*	*Gravel*	*0.2581*	*0.1666*	*6.00*	*4.16*	*13.82*	*0.0585*	*2.85*	*12.39*

* Those experimental data were obtained from the concrete sample size of 40×40×8 cm

** This values were taken from the uniformity test of concrete samples by means of ^{60}Co gamma-ray Transmission method.

efficiency.

For each test sample, the percent standard deviation in the uniformity as determined from measurements at 49 points was obtained and is shown in the last column of Table 3.

Except for some cases such as sample numbers, SM-1, SM-2 and MG-2 in this table, it is seen that all of the samples have nearly the same uniformity. Excluding those samples which showed large deviation, the others were taken for a study of the gamma-ray shielding effect in detail.

The average linear-absorption coefficient was obtained by the same way as mentioned above and is shown in Table 3.

Data for the transmission ratios, subdued lengths, 1/10 values lengths, half-value lengths, mass absorption coefficients and overall densities measured are included in Table 3. For comparison, the experimental data was obtained for some concretes which were in part made up of materials different from the magnetite of interest, such as sample numbers, SM-1, SM-2, MG-1 and MG-2. Samples M-8 and M-9 are concretes manufactured by using a grain of up to 0.6 mm diameter (from the grain curve "a" on Fig. 1) as a fine aggregate.

3. Data Analysis

As discussed before, the attenuation of gamma radiation in materials is mainly caused by photoelectric effect, Compton scattering and pair production. Photoelectric effect and pair production in radiation shielding calculations can be interpreted with sufficient accuracy as simple absorption due to the short mean free path of the secondaries. In Compton scattering the electrons of the atomic shells absorb only a part of the energy of the photons. A considerable fraction of the primary photons continue with diminished energy further into the shield at an angle deviating from the original direction.

Among the emergent photons from the shield surface, almost all of the sacttered photons are from Compton scattering in the case of the Co-60 gamma-ray and of the magnetite heavy concrete under consideration.[7,8] Although characteristic X-rays can be produced by photoelectric effect and pair production the photon yield due to them appear be negligible compared to those from Compton scattering.

The energy of the photons produced by the Compton scattering, E, is given by the equation.

$$E = \frac{E_0}{1+\frac{E_0}{0.511}(1-\cos\theta)} \quad \cdots\cdots\cdots\cdots\cdots\cdots(1)$$

were E_0 is the primary energy in Mev and θ is the scattering angle. According to Eq. (1), the scattered photons have an angular distribution which depends on the differential Compton scattering cross section. The Klein-Nishina formula for the angular distribution function of the scattered photons per steradian of solid angle may account for the fact that the scattered photons have a radial distribution with pronounced forward direction. If so, the photon flux with high energy may be predominantly high compared to that with low energy in the direction of perpendicularly incident photon to the slab sample, even if the emergent scattered photons have the energy distribution over a wide energy region. This is the case only for the single scattering of photons but in the case of multi-scattering, the spectrum of the scattered photons cannot be easily interpreted by the formula.

Nakata et al.[9] measured the energy distribution of back scattered gamma-rays from lead, iron and ordinary concrete slabs using Co-60 and Cs -137 gamma-ray sources. They found that the backscattered photons from a concrete wall are made up from multi-scattered

rays, while backscattered rays from a lead slab consist mainly of single scattered photons and characteristic X-rays. From their conclusion, it may be stated that a significant distortion from the spectrum predicted by the Klein-Nishina formula will be noted in the actual emergent spectra, owing to the multi-scattering process of gamma-radiation in concrete. Therefore, if the spectra of the emergent photons vary as the thickness of the concrete shield is varied, an attenuation curve should be obtained upon analysis of the experimental data under consideration.

The response of the NaI Scintillation detectors depends on the energy of radiation.[10, 11] This presents another difficult problem in interpreting the experimental data accurately. In the measurement of gamma radiation with a Scintillation detector, a fraction ε (efficiency) of the incident photons produce flashes of light which are converted into electrical current pulses by photocathodes and secondary multipliers. The efficiency. $\varepsilon(E)$, of a scintillation crystal for a normally incident photon is obtained by the equation.

$$\varepsilon(E)=1-e^{-\mu(E)d} \quad \cdots\cdots(2)$$

in which $\mu(E)$ is the attenuation coefficient of sodium iodide as a function of energy in Mev and d is thickness of the scintillation crystal. $\varepsilon(E)$ describes the probability of any interaction of the photons penetrating the crystal to lead to a recording of a current pulse.

If the true emergent spectrum is known, the pulse count rate (in cpm or cps) by detector in question will be easily obtained by

$$R=\int_0^{E_{max}} \phi(E)\ \varepsilon(E)\ dE \quad \cdots\cdots(3)$$

Here R is pulse count rate in cpm or cps, $\phi(E)$ is radiation flux as a function of energy and E_{max} means the energy of the primary radiation.

The pulse height spectrum of the emergent photons from the concrete shield obtained by a multi-channel analyzer, is not the true spectrum. The true spectrum consists only of the primary and secondary radiations produced in the shield medium. The spectrum of photons produced in the detector itself is not usually that of the emergent photons. This makes a reliable interpretation of the experimental data extremely difficult.

In the first approximation, it is, therefore, assumed that the spectral distribution produced by the uncollided photons is the same as that produced by the primary photons when no absorber is placed between the radiation source and the detector. A further assumption was made that the emergent scattered photons from the shield surface are attenuated only by the absorption in the crystal.

The variation of the emergent spectra using a 3 in. diameter by 3 in. long NaI(Tl) scintillation crystal associated with 400 multi-channel analyzer (Hitachi, model RAH-403). These data obtained with changing concrete shield thickness are shown in Fig. 3.

Compton scattered photons produced by the uncollided primary photons are included in these spectra except for the primary photons shown in the upper part of this figure. When analyzing the data, this uncollided primary portion was subtracted from each curve.

Thereby, the remaining part may be said to be the emergent scattered photons from the shield surface.

From these results, the response variation of the NaI(Tl) crystal to the different spectra were calculated on the basis of the work of Grosjean.[11] For our purpose, the relative efficiency variation was calculated as a function of the concrete shield thickness. The results are presented in Table 4 and Fig. 4.

All the counting data were corrected and analyzed by the factors given above.

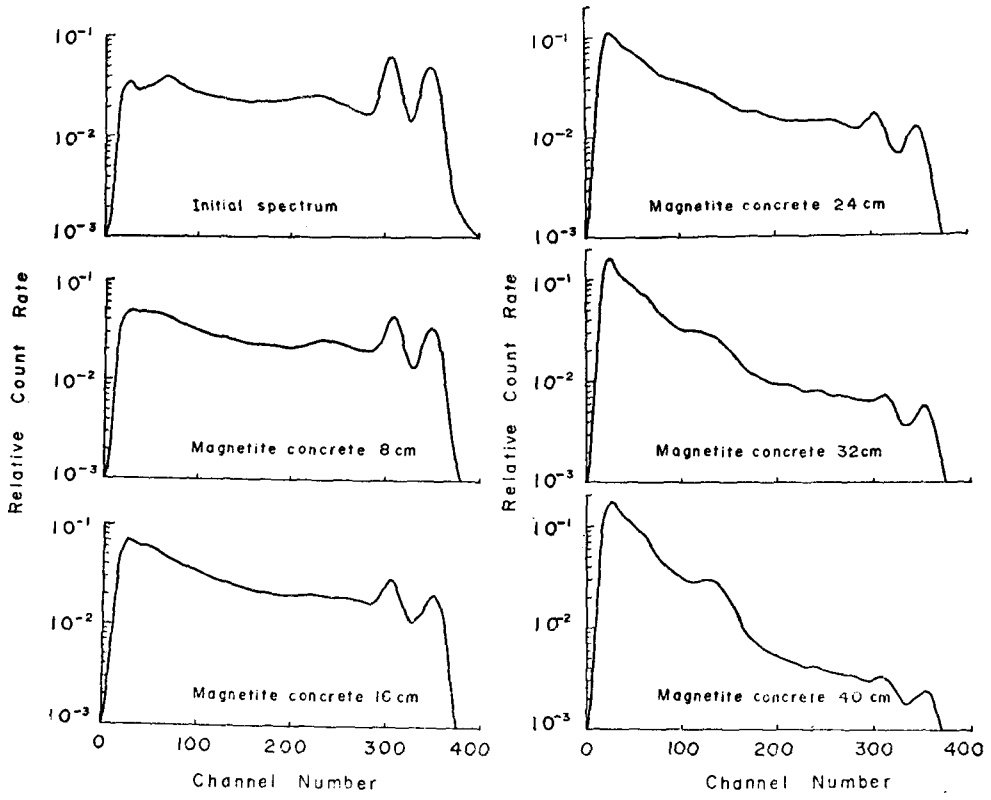

Fig. 3. Variations of pulse height spectra with magnetite concrete thickness.

Table 4. Magnetite concrete thickness Vs. relative counting efficiency

Magnetite concrete thickness(cm)	Relative counting efficiency
0	1.00
8	1.12
16	1.38
24	1.69
32	1.81
40	1.85
48	1.88

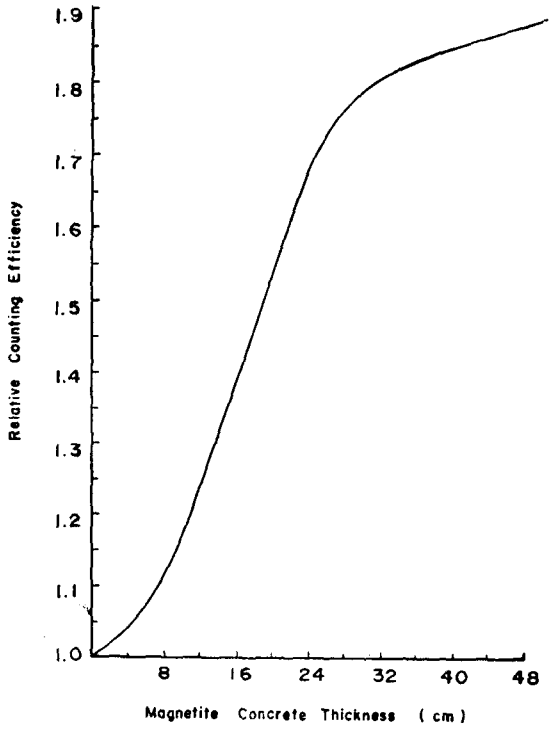

Fig. 4. Relative counting efficiency of NaI(Tl) crystal as a function of magnetite concrete thickness.

4. Results and Discussions

A typical attenuation curve of Co-60 gamma -ray in the magnetite heavy concrete is shown in Fig. 5. In this figure, the observed transmission rate against the concrete shield thickness was plotted together with that corrected according to Eq. (3). For comparison, the

data obtained by the narrow beam are included in Fig. 5.

For the sake of convenience a mathematical expression governing the relation between the transmission ratio and thickness of shielding concrete was derived from a polynomial fitting of the experimental data. The best curve fit is the third degree polynomial,

$$\log_{10} I_{(x)}/I_{(o)} = -4\times10^{-2}X - 1.47\times10^{-3}X^2 + 2.3\times10^{-5}X^3 \cdots\cdots(4)$$

Here $I_{(x)}$ is radiation intensity after passing through a thickness X of absorber, $I_{(o)}$ is the initial radiation intensity and X is the thickness of absorber. This empirical formula is applicable for the magnetite heavy concrete with a density of about 3.5 g/cm^3 and the concrete shield thickness up to 20 cm. For the concrete shield thicker than 20 cm, the above empirical formula is not fitted well. So the following formula was obtained using a least squares fittings of the experimental values for concrete thickness greater than 20 cm.

$$\log_{10} I_{(x)}/I_{(o)} = -6.45\times10^{-2}X + 9.22\times10^{-2} \cdots(5)$$

Here all the symbols are the same as described above.

If the above equations are rewritten to include the typical formula for the radiation attenuation in the magnetite heavy concrete with a linear attenuation coefficient of about 0.195 cm^{-1}, They become

$$I_{(x)}/I_{(o)} = \exp(-0.195X)\ \exp(1.03\times10^{-1}X - 3.38\times10^{-3}X^2 + 5.29\times10^{-5}X^3) \cdots\cdots(6)$$

when X<20 cm,

$$I_{(x)}/I_{(o)} = \exp(-0.195X)\exp(4.66\times10^{-2}X + 2.12\times10^{-1}) \cdots\cdots(7)$$

when X>20 cm.

On the right side of Eqs. (6) and (7), the first exponential factors in the formulae mean attenuation of the primary photon and the second factors are for the scattered photons produced in a shield medium. Second exponential factors may be called the build-up factor.

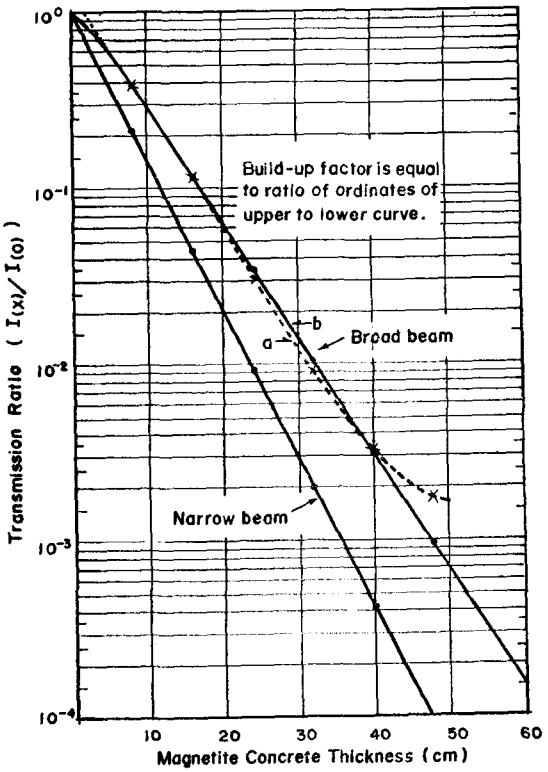

Fig. 5. Magnetite concrete thickness Vs. transmission ratio for ^{60}Co gamma.

*** a: indicates polynomial fittings**
b: indicates least squares fittings

The build-up factors obtained experimentally in this study are given for a various thickness of magnetite concrete shield having a density of 3.5g/cm^3 in Table 5.

Table 5. Build-up factors for various thickness of magnetite concretes

Magnetite concrete thickness (cm)	Build-up factor
8	1.83
16	2.58
24	3.76
32	5.31
40	7.95
48	11.36

The above equations, Eqs. (6) and (7), can be written in the generally used attenuation formula of broad beam source, $I_{(x)}/I_{(o)} = e^{-\mu x}\cdot B$.

Here μ is the linear attenuation coefficient and B refers to the build-up factor. In this way, Eqs. (6) and (7) may be expressed by generalized forms.

$$I_{(x)}/I_{(o)}=\exp(-\mu X)\ \exp(1.03\times10^{-1}X - 3.38\times10^{-3}X^2+5.29\times10^{-5}X^3) \quad \cdots\cdots(8)$$

when $X<20$ cm,

$$I_{(x)}/I_{(o)}=\exp(-\mu X)\ \exp(4.66\times10^{-2}X+ 2.12\times10^{-1}) \quad \cdots\cdots(9)$$

when $X>20$ cm.

Where $\mu=0.0532\rho+0.0083$ $\cdots\cdots(10)$

The relationship (Eq. 10) between μ and ρ was obtained for the magnetite concrete in the earlier work.[4] These empirical formulae [Eqs. (8) and (9)] can be used for magnetite concrete with densities(ρ) ranging from 2.7 to 3.8 g/cm^3.

Among the emergent photons, the primary radiation will proportionally decrease while the secondary radiation will increase with adding to shield thickness. This may account for that the primary photons decrease exponentially, but the secondary photons will increase due to scattering as the shield thickness increase. When the shield thickness is about 6 times the mean free path (5.1cm for the heavy concrete under investigation), the emergent photons may be predominated by the secondary radiation produced in the shielding material. If more shield is added, a decrease of the emergent photon flux will follow the usual attenuation law with a absorption coefficient relative to the secondary radiation. Accordingly a linearity between the shield thickness and the transmission ratio will be found on in a semi-log paper, and such a tendency is clearly shown in Fig. 5. One may say it is dangerous to assume the linearity in the range $\mu X>6$. This may be explained by the fact that photoelectric reaction by photons with low energy is dominant in the magnetite concrete used here in this study, leading to insignificant build-up effect by the secondary radiation.[12]

The validity of the experimental results obtained here in this work is unable to be examined because no data for the magnetite heavy concrete obtained experimentally or theoretically by other investigators are available. But the values for ordinary concrete calculated by the empirical formulae [Eqs. (8) and (9)] obtained in this work was in reasonable agreement with the data given in the reference.[13]

According to the previous study, it was revealed that natural aggregate concretes cost about \$ 6.5/m^3 for materials. Using magnetite aggregate, densities from 3.9~4.27 g/cm^3 can be otbained at \$ 36~\$ 40/m^3 for materials. This concrete material cost is about 6 times cheaper than that of lead ore aggregate concrete heaving aggregate density of 4.7g/cm^3 and concrete density of 3.6g/cm^3.

In addition, the emergent radiation flux obtained in the magnetite concrete box type shield model amounted to about 1.08 times that of the slab shield. This increase may come from the backscattered radiation. This result implies that the data on the shielding effect, which were obtained on slabs or one-sided shields and are usually presented in the references[3, 12], can not be used directly in practical shielding calculation. In other words, the biological shield should be designed taking into account this phenomenon.

5. Conclusion

The gamma-ray shielding effects of magnetite heavy concretes which are readily and economically available in domestic market have been investigated by means of a broad beam ^{60}Co gamma-ray source. Summing up this study, the results are as follows;

1). Magnetite seems to be the most promising aggregate material among mineral ores used in this study because magnetite has a relatively

high density of 4.25g/cm³ in average, a good physical strength as well as economical and readily avialable in domestic market. A concrete in density of about 3.5g/cm³ with a good physical strength has been obtained by mixing up coarse aggregate of magnetite with magnetite fine aggregate of about 54% iron elements.

2). From the experimental data, the empirical formulas were derived governing the relationship between the transmission ratio and the shield thickness for magnetite concrete with the densities between 2.7 and 3.8g/cm³ and are

$I_{(X)}=I_{(O)}\exp(-\mu X)\exp(1.03\times10^{-1}X-3.38\times10^{-3}X^2+5.29\times10^{-5}X^3)$

when $X<20$ cm,

$I_{(X)}=I_{(O)}\exp(-\mu X)\exp(4.66\times10^{-2}X+2.12\times10^{-1})$

when $X>20$ cm,

in which μ is given by $(0.0532\rho+0.0083)$.

3). The shielding effect in a model box type shield constructed in this experiment amounted to about 0.92 times of that of the slab shield.

Acknowledgment

The author wishes to express his thanks to professor P. Y. Pac the Dept. of Nuclear Eng. Seoul National University for his continual encouragement and thanks to Mr. S. G. Ro, Mr. J. C. Lee and Mr. S. H. Cho, the Health Physics Division, AERI. ROK for their assistance in carrying out the experiments. Thanks are also due to Mr. S. M. Kim, Chief, the Material Testing Section, National Construction Research Institute for his kind help in compressive testing of concretes and to Mr. S. K. Yoon, Chief, the Geological Chemistry Section, Geological Survey of Korea for the chemical analysis of mineral ore.

References

1) D. E. Starchman and F. E. Hoecker, Health Physics, Vol. **20**, No. 1, pp. 49~53, (1971)
2) Y. Furuta, A. Tsuruo, S. Miyasaka, K. Tamura and Y. Kanemori, Nuclear Science and Engineering, **25**, pp. 85~92, (1966)
3) T. Rockwell, Reactor Shielding Design Manual, lst. Ed., pp. 447~450, D. Van Nostrand Co., Inc,, New York, 1956.
4) Yong Kyu Lim, Gamma-radiation Shield Effect of Various Heavy Concretes Using Domestic Mineral Aggregates, Journal of the Korean Nuclear Society, Vol. 2, No. 3, pp. 149~161, September 1970.
5) J. Certaine, Augular Distribution of Photons from Plane Monoenergetic Sources, NYO-3074, pp. 41~48, 1953.
6) W. Futtermenger, A Method for the Measurment of Increment Factors for Gamma-radiation in the Energy region of 0.5~15 Mev, ORNL-tr-1869 or ABS-THH-1019, pp. 3~19, 1966.
7) Goldstein and J. E. Wilkins, Jr., Calculations of the Penetration of Gamma-rays, NYO-3075, pp. 60~63, 1954.
8) H. Goldstein, Fundamental Aspects of Reactor Shielding, pp. 140~159, Addison Wesley Publishing Co. Inc., Massachusetts (1959).
9) M. Nakata, T. Fuse and K. Takeuchi, J. Transport. Tech. Res. Inst. pp. 561~568, **11** (1961).
10) R. L. Heath, Scintillation Spectrometry, Gamma-ray Spectrum Catalogue, TID-4500. 13th Ed., pp. 18~19, July 1, 1957.
11) C. C. Grosjean and W. Bossaert, Table of Absolute Detection Efficiencies of Cylindrical Scintillation Gamma-ray Detectors, Computing Laboratory of the University of Ghent, Ghent, Belgium, pp. 305~306, 1965.
12) R. G. Jaeger, E. P. Blizard, A. B. Chilton, M. Grotenhuis, A. Hönig, Th. A. Jaeger and H. H. Eisenlohr, Engineering Compendium on Radiation Shielding, Shielding Fundamentals and Methods, pp. 167~233, Springer-Verlag, Berlin, 1968.
13) Radiological Health Handbook, U. S. Dept. of Health, Education, and Welfare, Public Health Service, p. 149, January 1970.